Chapter 3

SYNTHESES AND BEHAVIOR STUDIES OF ORGANIC AMMONIUM CHLORIDE SALTS (OACSs)

Abstract

In this chapter we describe syntheses and characterization of twenty two organic ammonium chloride salts (OACSs). The studies on OACSs using TG/DTA, DSC measurements and temperature dependent Raman study showed interesting solid-solid phase transitions. DSC measurement for anilinium chloride has shown solid-solid phase transition around 260 K. Examination of DSC proved that absence of solid-solid phase transition after addition of any substituent on aromatic ring (except 3-nitro anilinium chloride) in OACSs. To confirmed solid-solid phase transition of anilinium chloride we have carried out temperature dependent Raman study. Raman spectra proved that pure crystalline anilinium chloride undergoes two order-disorder phase transitions, one at 260 K and other between 300 K - 350 K. The Raman study for 4-nitro anilinium chloride showed one phase transition between 260 K - 300 K, which not observed in DSC measurement. These solid-solid phase transitions are reversible in nature and can be repeated for cycle.

3.1 Introduction

Ammonium salts can be prepared by reacting organic amines with mineral acids [1]. Smaller ammonium salts, methyl ammonium, has size comparable to alkali and alkaline earth metal ions. This property is explored in solid state chemistry to prepare variety of solid solutions, or compounds that includes perovskites of the type AMX_3, A_2MX_4 etc [2,3]. Apart from this, ammonium salts show independently solid-solid to phase transitions [4]. These are well studied in literature using spectroscopic techniques, powder X-ray diffraction and thermal analysis [5,6]. These salts are also well studied for 'polymorphic' behavior in literature [7]. In this chapter we have restricted investigation of ammonium chloride salts only. This involves synthesis/preparation and characterization of series of organic ammonium chloride salts (OACSs). We studied OACSs for solid-solid phase transitions using TG/DTA, DSC measurement, and temperature dependent Raman spectroscopy. These salts are building blocks for making organic-inorganic hybrid compounds (OIHCs), a theme of the thesis.

3.2 Experimental

3.2.1 *Materials and methods*

All chemicals and solvents used were of analytical grade reagents. Aniline, benzyl amine, methyl amine (40 %), *n*-propyl amine and *n*-butyl amine (s. d. fine); 3-nitro aniline and 4-nitro aniline (spectrochem); 4-fluoro aniline (chemport); 3-chloro aniline, 4-chloro aniline, 4-chloro benzyl amine, (*R*)- and (*S*)-methyl benzyl amine, (*R*)- and (*S*)-4-chloro methyl benzyl amine, (*R*)- and (*S*)-ethyl benzyl amine, (*S*)-2-butyl amine, ethyl amine, (*R*)- and (*S*)-1,2-diamino propane dihydrochloride, 1,3-diamino propane, 2-adamantanamidinium chloride and 2-amino benzothiazole (Aldrich); 1,2-dimino ethylene and conc. hydrochloric acid (qualigens) and ethyl alcohol (Baroda chemicals) were used without any further purification.

3.2.2 Syntheses of OACSs

A series (twenty two) of OACSs were prepared by slow neutralization of ethanolic solutions of organic amine with appropriate ethanolic solution of conc.

hydrochloric acid in 1:1 molar ratio at room temperature (RT). We obtained good quality of crystal after placing this solution at RT for significant numbers of days. The nitro-anilinium chlorides were obtained by refluxing appropriate ethanolic mixture of nitro-aniline and conc. hydrochloric acid in 1:1 ratio at 351 K. After refluxing the resulting solution for 2 - 3 hours it was placed at RT and was left undisturbed for about a week after which we obtained the good quality crystals of nitro-anilinium chloride within a week. Recrystallization was also performed to increase the purity of all crystals. A general methodology of OACSs preparation/syntheses is mentioned in scheme-I.

Scheme-I

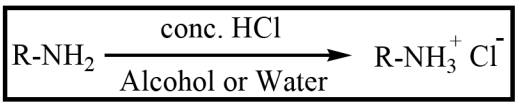

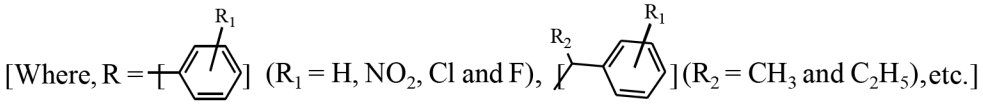

$-CH_3$, $-C_2H_5$, $-C_3H_7$, $-C_4H_9$, etc.

Actual process for synthesis of anilinium chloride; 10 mL (109.7 mmol) of aniline was taken in beaker containing 100 mL of ethanol then added 14.9 mL (142.7 mmol) of conc. hydrochloric acid. The resulting solution was stirred for few minutes and then kept at RT, exposed to air. After 3 - 4 hours crystals of anilinium chloride were collected and filtered.

Yield: 80 - 90 %

The formations of OACSs were confirmed by FT-IR spectra, ^{1}H NMR analyses and thermal analyses.

3.3 Results and Discussions

3.3.1 General Discussion

Crystal structure of ammonium chloride at RT was reported by Goldschmidt and Hurst in 1951 [8]. XRD of ammonium chloride at RT has shown the structure to be of CsCl type. It is crystallized in cubic crystal system, space group symmetry T_d, with N-

H links of ammonium ion directed essentially towards four of the eight surrounding chloride ions [9]. By replacing one hydrogen atom of ammonium ion with organic group, one gets compounds which can be further divided into two categories on the basis of their crystal structure as shown in Chart 3.1.

Chart 3.1 Structural Change by substitution

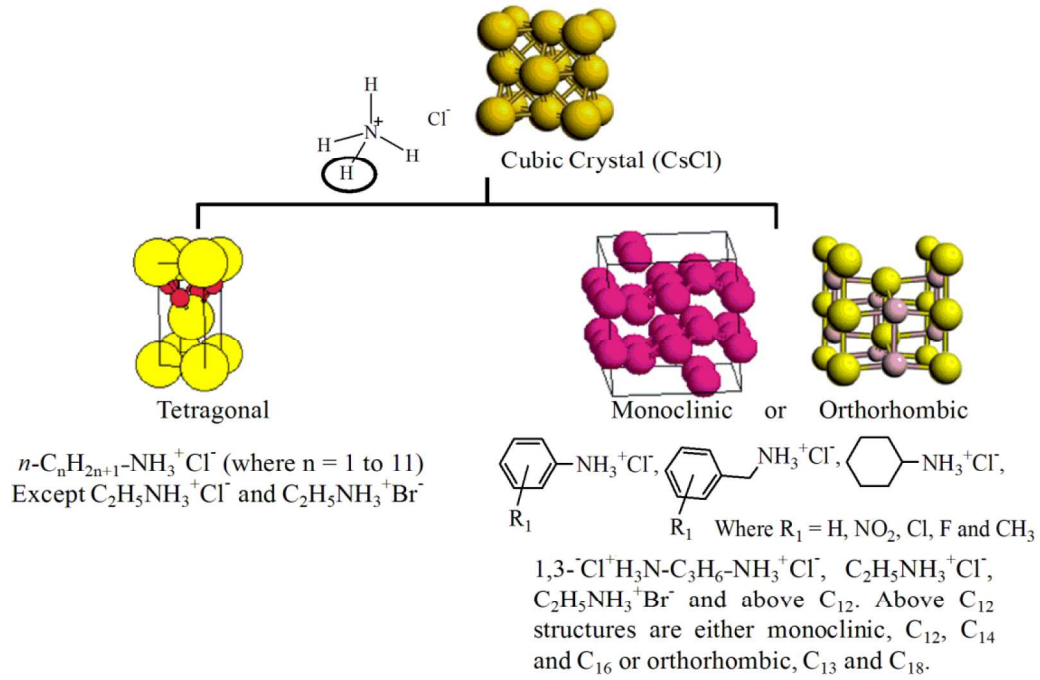

First category contains tetragonal crystal structure, while second category contains monoclinic or orthorhombic structures. A series of *n*-alkyl ammonium halides (C_1 to C_{11}) come in the first category. It has C-N axis coinciding with fourfold crystallographic axis (space group: D_{4th}^7-*P4/nmm*), where every nitrogen atom is surrounded by four chloride ions with two molecules per unit cell. This clearly indicates that ions are at D_{2d} or C_{4v} symmetry sites. In order to reconcile the fourfold symmetry of the ions, the ions must randomize their orientation either by the rotation or by orientational disorder. Literature cited all *n*-alkyl ammonium halides generally crystallize in tetragonal structure up to C_{10} except for ethyl ammonium chloride and bromide which are monoclinic [10,11]. The *n*-alkyl ammonium halide up to C_{16} except ethyl ammonium chloride has shows the structural transitions at LT and/or HT, which were studied using crystal structure by thermal analyses and spectroscopic techniques [12]. The structural transition in *n*-alkyl ammonium chloride is, due to the

rotation of the cations [13]. Tsau and Gilson determined the enthalpies and transition temperatures for a series of halide salts, *n*-alkyl ammonium halides (C_1 to C_{16}); from 123 K to their melting point temperature [14].

Second category contains ethyl ammonium halide, cyclohexyl ammonium halide [15] and above C_{12} [16]; 1,3-diammonium propane dichloride; anilinium chloride, 3-nitro anilinium chloride [17]; 4-nitro anilinium chloride [18]; 4-chloro anilinium chloride [19]; 4-chloro benzilinium chloride [20]; 4-methyl anilinium chloride [21].In most of the second category salts every nitrogen atom is surrounded by only three halogen ions the remaining molecules in the crystal lie on general or fixed positions. The crystal structure of anilinium chloride at RT was determined by Brown using single crystal XRD technique [22]. It has monoclinic structure with three chloride ions surrounding the $-NH_3^+$ group and has four molecules per unit cell (space group: C_s^4-C_c). Alkyl ammonium halides C_{12} to C_{16} shows a clear phase transition in thermal analysis, while anilinium chloride, 4-fluoro anilinium chloride, 4-chloro anilinium chloride, 3-chloro anilinium chloride, 4-nitro anilinium chloride, 4-chloro benzilinium chloride, (*R*)- and (*S*)-4-chloro methyl benzilinium chloride, (*S*)-2-butyl ammonium chloride, 2-amino benzothiazolinium chloride and 2-adamantanamidinium chloride along with ethyl ammonium chloride and cyclohexyl ammonium halides have not shown clear structural phase transition [12,23]. The LT form of *n*-propyl ammonium chloride is monoclinic [24]. It turns out that LT phases of halides belonging to the first category compounds have crystal structure similar to ambient temperature crystal structure of the organic ammonium halides belonging to the second category while the second category compounds do not show signature of structural phase change at all. Therefore, anilinium chloride and ethyl ammonium chloride have not shown any clear cut structural phase transition, neither there is strong spectroscopic nor thermal evidence. But in disordered materials the molecular groups on certain lattice sites undergo hindered rotations in the prototype phase. On lowering temperature these hindered rotations freeze and the system undergoes an order-disorder phase transition. The Raman spectroscopy in such transitions provides useful information [25,26]. Ammonium halides undergo a number of order-disorder phase transitions with respect to the orientation of ammonium ions [7]. We have undertaken a systematic temperature dependent Raman spectroscopic to examine for anilinium chloride in view of this controversy.

3.3.2 FT-IR spectra

FT-IR spectra for a series of OACSs were recorded in the range of 4,000 - 400 cm^{-1} at RT. After hydro-chlorination of organic amines, the broad bands are appear in almost all the OACSs in the region 3250 - 2600 cm^{-1} are indication of the formation of hydrochloride salts [27]. The details of infrared spectroscopy for a series of OACSs are specified in Table 3.1. The broad bands in the region 3250 - 2600 cm^{-1} for the chloride salts contains the N-H ($R\text{-}NH_3^+$) stretching vibrations were observed due to the continuous series of overlapping bands, combination and overtone bands. The intense band about 2550 cm^{-1} can be resolved into two features at 2575 cm^{-1} and 2550 cm^{-1}. These two features about 2550 cm^{-1} are assigned to the Fermi resonance processes corresponding to combination bands of N-H ($R\text{-}NH_3^+$) deformation modes and N-H ($R\text{-}NH_3^+$) rocking modes [27]. The combination band at 1494 cm^{-1} and 1055 cm^{-1} are assigned anti-symmetric N-H ($R\text{-}NH_3^+$) deformation and rocking respectively. The combination band at 1437 cm^{-1} and 1118 cm^{-1} are assigned symmetric N-H ($R\text{-}NH_3^+$) deformation and rocking respectively [1,27]. The bands also observed at 1220 - 1020 cm^{-1} due to aliphatic C-N stretching and 1340 - 1250 cm^{-1} due to primary aromatic C-N stretching. The other mode which provide vital information about the aromatic C-H out of plane deformation; the two bands were observed between 770 - 730 cm^{-1} and 710 - 690 cm^{-1} for five adjacent hydrogen atoms, 810 - 750 cm^{-1} for three adjacent hydrogen atoms and between 860 - 800 cm^{-1} for two adjacent hydrogen atoms [Figure 3.1 (a)]. The other bands were observed around 1066 cm^{-1} and 642 cm^{-1} for aromatic C-F and C-Cl stretching respectively (Figure 3.1 (b)). The two bands at 1554 - 1503 cm^{-1} and 1352 - 1338 cm^{-1} is due to N=O asymmetric and symmetric vibration for nitro-anilinium chloride (Figure 3.1 (c)). The bands observed between 1486 cm^{-1} to 1454 cm^{-1} in the spectrum of benzilinium chloride, (*R*)- and (*S*)-methyl benzilinium chloride, (*R*)- and (*S*)-ethyl benzilinium chloride and for alkyl ammonium chloride deformation of the CH_2 and CH_3 group (Figure 3.1 (d) and (f)) [28]. The bands observed at 1411 cm^{-1} for methyl ammonium chloride is due to the C-H deformation in CH_3-N as shown in Figure 3.1 (h). In case of 2-amine benzothiazolinium chloride and 4-chloro benzilinium chloride bands also observed at 3395 cm^{-1} and 3324 cm^{-1} due to N-H stretching mode of NH_2 and H_2O respectively as shown in Figure 3.1 (e) and (g). For the hydrogen bond (N-

H···Cl) bands were observed around 2017 cm^{-1} and 1395 cm^{-1} owed stretching mode and deformation mode almost all the OACSs [29].

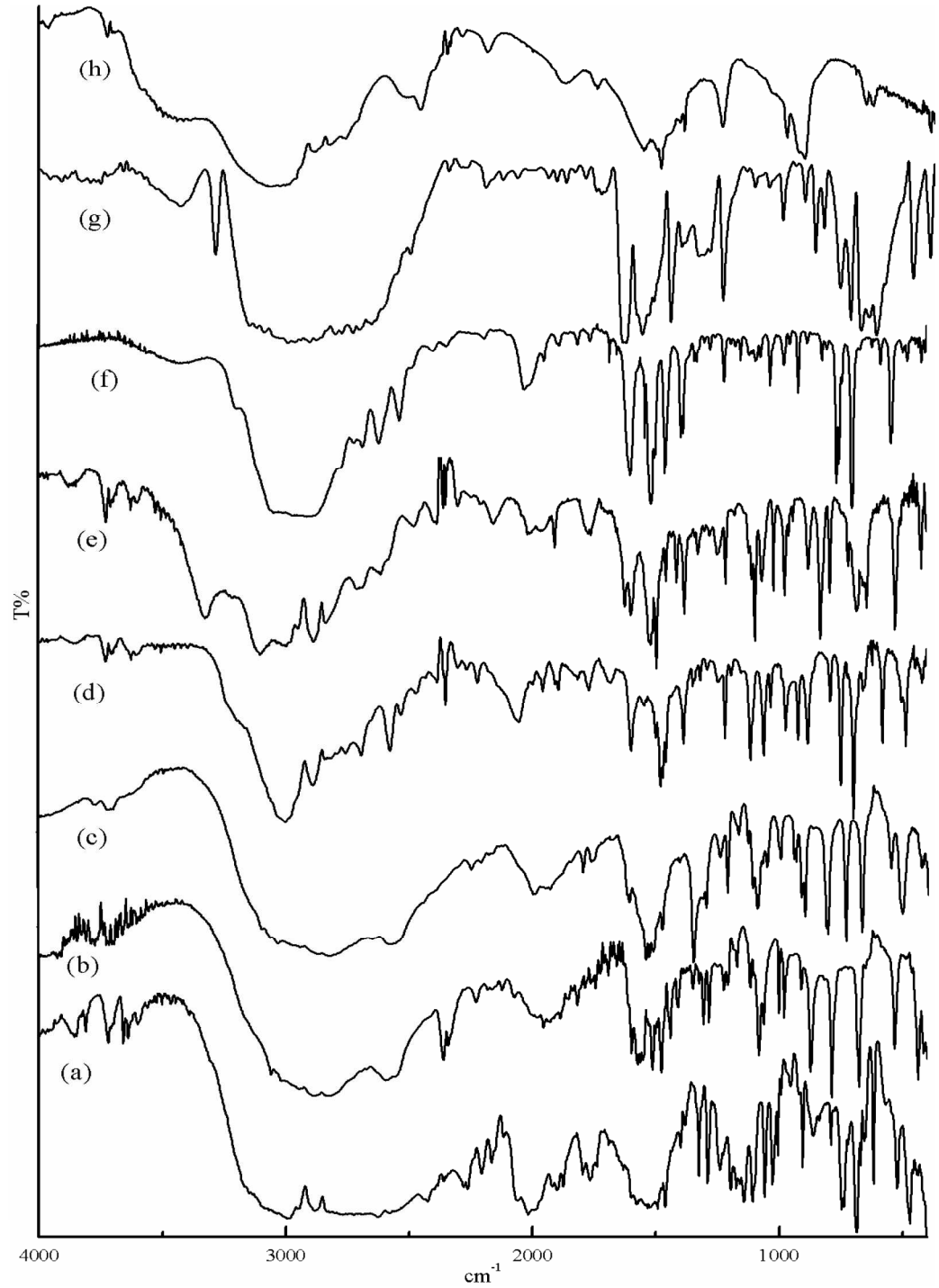

Figure 3.1 FT-IR transmission spectra of anilinium chloride (a); 3-chloro anilinium chloride (b); 3-nitro anilinium chloride (c); benzilinium chloride (d); 4-chloro benzilinium chloride (e); (*R*)-ethyl benzilinium chloride (f); 2-amine benzothiazolinium chloride (g) and methyl ammonium chloride (h).

Table 3.1 FT-IR spectra of organic ammonium chlorides salts at room temperature. All frequencies are given in cm^{-1}

Compounds	NH_3^+ str.	$^+N–H\cdots Cl$ H-bond	NH_3^+ def. & rocking	C=C str.	C–H def.	C–N str. & C–C def.	=C-H in plane def.	=C-H out of plane def.	N=O str.	C–Cl or C-F str.
Ammonium Chloride	3104vs, 3028s, 2819s	2017s, 1385vs	1548s, 1065w							
Anilinium chloride	2994vs, 2626vs	2058s, 1400m	1632s, 1536vs, 1107s, 1060s,	1601s, 1580s, 1500s, 1461s		1289s, 991w	1196vs, 1175s, 1160s, 1140s, 1027s	746vs, 695vs		
4-Fluoro anilinium chloride	2856vs, 2613s	2017s, 1395s	1626s, 1103s, 1066s	1602m, 1568s, 1504vs		1299s	1207s, 1183w, 1160s	831vs		1021s
4-Chloro anilinium chloride	2855vs, 2604vs	2015s	1640m, 1543s, 1113s	1593s, 1563s, 1490vs, 1415s		1309s	1205s, 1172m, 1145s, 1015s	820vs		637s
3-Chloro anilinium chloride	2887vs, 2596s	2073m	1642w, 1549s, 1116m, 1063s	1599s, 1574s, 1502s, 1440s		1308s	1207w, 1171w, 1082s	787vs		674vs
4-Nitro anilinium chloride	3072m, 2886m	2003s	1640s 1533s 1115m, 1074w	1601s, 1584m, 1503m		1300s	1181m, 1135m, 1052m	843s	1548m, 1330m	
3-Nitro anilinium chloride	3036s, 2827vs, 2580sf	2001s, 1405w	1613s, 1532vs, 1111s, 1075w	1560s, 1458w		1300s	1213s, 1169w, 1130m, 1091s, 1053m	804s	1554vs, 1352vs	

Benzilinium chloride	2996vs, 2694s 2574sf	2051s, 1384s	1543m, 1113s, 1059s	1597s, 1498s, 1454s	1465s	1215s	1190w, 1151w, 1031m	746s, 695vs		
4-Chloro benzilinium chloride	3101vs, 2883s	2017w, 1381s	1622s, 1523s, 1117m, 1067m	1597s, 1494vs	1455s	1213s	1176w, 1094s, 1017s	831s		642s
(*R*)-Methyl benzilinium chloride	2879s, 2677s	2026s, 1385vs	1514vs, 1125w, 1066s	1607vs, 1502vs	1454s	1227s	1173w, 1090s, 1029s	764s, 698vs		
(*S*)-Methyl benzilinium chloride	2878s, 2676s	2033s, 1385vs	1515vs, 1126w, 1065s	1606vs, 1503vs	1454s	1227s	1173w, 1090s, 1029s	763s, 698vs		
(*R*)-4-Chloro methyl benzilinium chloride	2881vs 2674s	2013m, 1387s	1642w, 1526s, 1124w	1612m, 1586s, 1499s, 1450m	1469m	1225m	1175w, 1096s, 1012s	844s		642s
(*S*)-4-Chloro methyl benzilinium chloride	2880vs 2674s	2014m, 1386s	1653w, 1526s, 1125w	1613m, 1587s, 1497s, 1454m	1486m	1227m	1175w, 1097s, 1012s	843s		642s
(*R*)-Ethyl benzilinium chloride	2910vs, 2620s	2029m, 1394s, 1385s	1653w, 1540s, 1118m, 1072m	1600s, 1504s, 1456s	1460s	1218m	1152m, 1092m, 1032s	763vs, 700vs		
(*S*)-Ethyl benzilinium chloride	2904vs, 2535s	2029m, 1394s, 1385s	1653w, 1540s, 1118m, 1071m	1601s, 1504s, 1456s	1460s	1218m	1152m, 1093m, 1032s	763vs, 700vs		
2-Ammonium benzothiazole chloride	3002vs, 2667vs	2075w	1658vs, 1535s, 1070w	1601s, 1577s, 1503, 1453s		1305s	1124w, 1013m	740vs		

Methyl ammonium chloride	3073vs, 2830s	2017m, 1408s	1503vs	1411s	1046s
Ethyl ammonium chloride	3052vs, 2779m	2017m, 1399s	1628m, 1516m	1465s	1038w
1,2-Diammonium ethane dichloride	3007vs, 2588s	1404w	1589s, 1565s		1034vs
n-Propyl ammonium chloride	3034vs, 2971vs, 2687m	2032w, 1399m	1570s	1463w	1033m
1,3-Diammonium propane dichloride	3016vs, 2691s, 2561s	2019s, 1404s	1609s, 1543w, 1104s	1464vs	1190s
n-Butyl ammonium chloride	3012vs, 2671s, 2521s	2019m, 1398s	1611s, 1547w, 1500vs, 1075s	1460s	1164s
(*S*)-2-Butyl ammonium chloride	2973vs, 2534s	2011m, 1393s	1608s, 1546w, 1500s, 1138s	1463s	1211m

3.3.3 ^{1}H NMR Spectra

^{1}H NMR spectra of OACSs were taken in DMSO-d_6. The spectra were characterized by chemical shifts around δ = 10.43 and δ = 8.60 respectively for -NH_3^+ group of anilinium chloride, benzilinium chloride and their substituent. ^{1}H NMR spectra obtained for -NH_3^+ group shows down field broad signal, indicates formation of ammonium chloride salts (Figure 3.2). The signals were also observed between δ = 7.18 - 7.56 due to the aromatic protons. The signal observed around δ = 4.37 are for benzyl protons in benzilinium chloride and substituted benzilinium chloride salts. For (*R*)- and (*S*)-methyl benzilinium chloride signals analyzed around δ = 2.80 and δ = 1.51 indicates the benzyl proton and methyl group of benzyl protons. In case of (*R*)- and (*S*)-ethyl benzilinium chloride signals around δ = 1.80 and δ = 0.74 are indicates the ethyl protons on benzyl group. In case of aliphatic ammonium chloride broad signal was observed around δ = 8.15 for R-NH_3^+ protons, indicates that hydro-chlorination of aliphatic amine. Other signals around δ = 2.69 and δ = 1.60, δ = 0.88 indicate the CH protons of -NH_3^+ substituent and alkyl protons. The details of ^{1}H NMR spectra for the OACSs are discussed in Table 3.2.

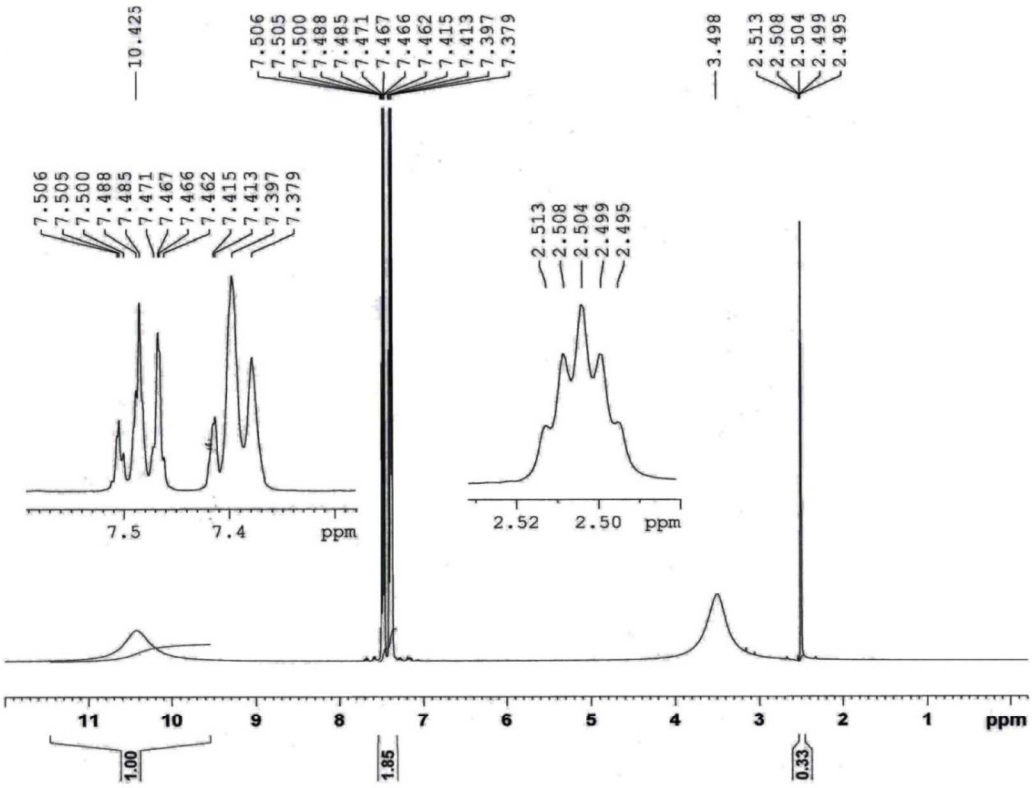

Figure 3.2 ^{1}H NMR spectra of anilinium chloride.

Table 3.2 ^{1}H NMR spectra of OACSs

Compounds	(δ value) ^{1}H NMR (DMSO-d_6) *J* coupling in Hz
Ammonium chloride	7.49 (s 4H, NH_4^+)
Anilinium chloride	10.43 (br s 3H, NH_3^+), 7.38–7.51 (m 5H)
4-Fluoro anilinium chloride	10.37 (br s 3H, NH_3^+), 7.42–7.46 (m 2H), 7.32–7.37 (m 2H)
4-Chloro anilinium chloride	10.06 (br s 3H, NH_3^+), 7.52 (d 2H, *J* = 8.4), 7.33–7.37 (m 2H)
3-Chloro anilinium chloride	10.58 (br s 3H, NH_3^+), 7.41 (t 1H, *J* = 8.0), 7.27 (d 2H, *J* = 8.8), 7.18 (d 1H, *J* = 8.4)
Benzilinium chloride	8.63 (s 3H, NH_3^+), 7.50-7.53 (dd 2H, *J* = 8.2), 7.34-7.43 (m 3H)
4-Chloro benzilinium chloride	8.52 (s 3II, NII_3^+), 7.48–7.55 (m 4II), 4.01 (s 2II)
(*R*)-Methyl benzilinium chloride	8.60 (br s 3H, NH_3^+), 7.53 (d 2H, *J* = 7.2), 7.42 (t 1H, *J* = 6.8, 7.6), 7.36 (t 2H, *J* = 7.2), 4.37 (q 1H, *J* = 6.8), 2.89 (s 1H), 2.73 (s 1H), 1.51 (d 3H, *J* = 6.8)
(S)-Methyl benzilinium chloride	8.60 (br s 3H NH_3^+), 7.53 (d 2H, *J* = 6.8) 7.42 (t 1H, *J* = 6.8, 7.6), 7.36 (t 2H, *J* = 7.2), 4.37 (d 1H, *J* = 6.8), 2.89 (s 1H), 2.73 (s 1H), 1.51 (d 3H, *J* = 6.8)
(*R*)-4-Chloro methyl benzilinium chloride	8.66 (br s 3H, NH_3^+), 7.57 (d 2H, *J* = 7.6), 7.50 (d 2H, *J* = 6.8), 4.41 (d 1H, *J* = 6.4), 1.50 (d 3H, *J* = 6.8)
(*S*)-4-Chloro methyl benzilinium chloride	8.58 (br s 3H NH_3^+), 7.55 (d 2H, *J* = 7.6), 7.50 (d 2H, *J* = 6.8) 4.41 (d 1H, *J* = 6.4), 1.49 (d 3H, *J* = 6.8)
(*R*)-Ethyl benzilinium chloride	8.70 (br s 3H, NH_3^+), 7.52 (d 2H, *J* = 7.2), 7.37–7.44 (m 3H), 4.09 (q 1H, *J* = 5.6), 1.99–2.05 (m 1H), 1.77–1.82 (m 1H), 0.73 (t 3H, *J* = 7.6 and 7.2)
(*S*)-Ethyl benzilinium chloride	8.63 (br s 3H, NH_3^+), 7.51 (d 2H, *J* = 7.6), 7.37–7.45 (m 3H), 4.09 (q 1H, *J* = 5.6), 1.99–2.02 (m 1H), 1.78–1.84 (m 1H), 0.74 (t 3H, *J* = 7.6 and 7.2)
2-Amino benzothiozilinium chloride	9.91 (s 2H, NH_2), 7.89 (d 1H, *J* = 7.6), 7.54 (d 1H, *J* = 7.6), 7.43 (dt 1H, *J* = 7.4 and 8.0), 7.29 (t 1H, *J* = 7.6 and 7.8), 4.67 (br s 1H, NH^+)
Methyl ammonium chloride	8.06 (s 3H, NH_3^+), 2.31 (q 3H, *J* = 5.6)
1,2-Diammonium ethane dichloride	8.49 (bs 3H, NH_3^+), 3.09 (s 2H)
n-Propyl ammonium chloride	8.15 (br s 3H, NH_3^+), 2.69 (s 2H), 1.52–1.62 (m 2H), 0.88 (t 3H, *J* = 7.6 and 7.2)
n-Butyl ammonium chloride	8.12 (br s 3 H, NH_3^+), 2.63–2.77 (m 2H), 1.49–1.57 (m 2H), 1.27–1.36 (m 2H), 0.87 (t 3H, *J* = 7.2)
(*S*)-2-Butyl ammonium chloride	8.06 (br s 3H, NH_3^+), 3.04 (s 1H), 1.58–1.68 (m 1H), 1.39–1.50 (m 1H), 1.16 (d 3H, *J* = 6.8), 0.89 (t 3H, *J* = 7.6)

3.3.4 Raman Spectra

Anilinium chloride crystallizes in monoclinic space group C_c with cell dimensions a = 15.84(3) Å, b = 5.33(3) Å, c = 8.58(3) Å, β = 101.10(2) and Z = 4 at ambient temperature. The benzene ring stack together as tightly as possible leave the chloride ions to arrange themselves equidistantly from as many nitrogen atoms as possible, which in this case only three see Figure 3.3. Consequently, every internal mode of anilinium ion has corresponding infrared and Raman active components in the lattice. Our studies have shown a broad agreement with the previous report on monoclinic type structures [30]. Figure 3.4 show three Raman modes at 168 cm^{-1}, 273 cm^{-1} and 400 cm^{-1} in the low frequency region, at RT. These modes are observed due to the liberations of anilinium ion. These modes are intense in the lattice mode region and carry important information about dynamics of the transition. By lowering the temperature, we observed decrease in the background noise, Rayleigh scattering. The modes at 168 cm^{-1} and 273 cm^{-1} show clear peak splitting and non-linear increase in the frequency as the temperature is lowered below 260 K, distinguish in Figure 3.5. These changes are reversible in nature and can be repeated without any change.

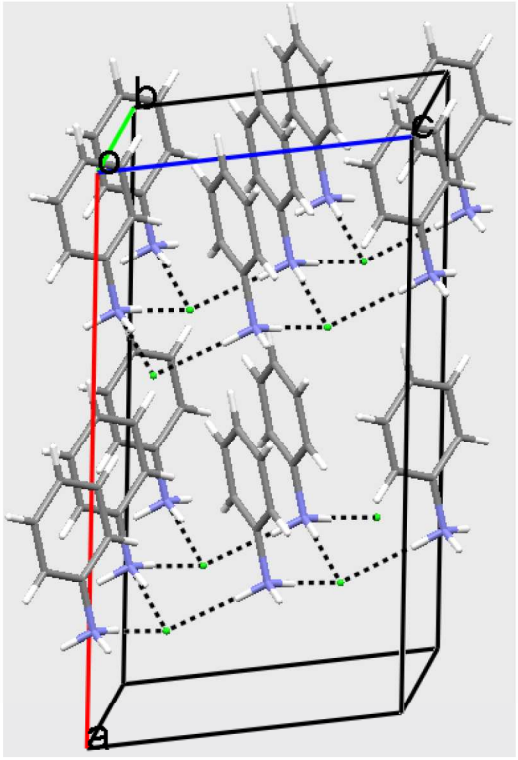

Figure 3.3 Packing and hydrogen bonding in anilinium chloride.

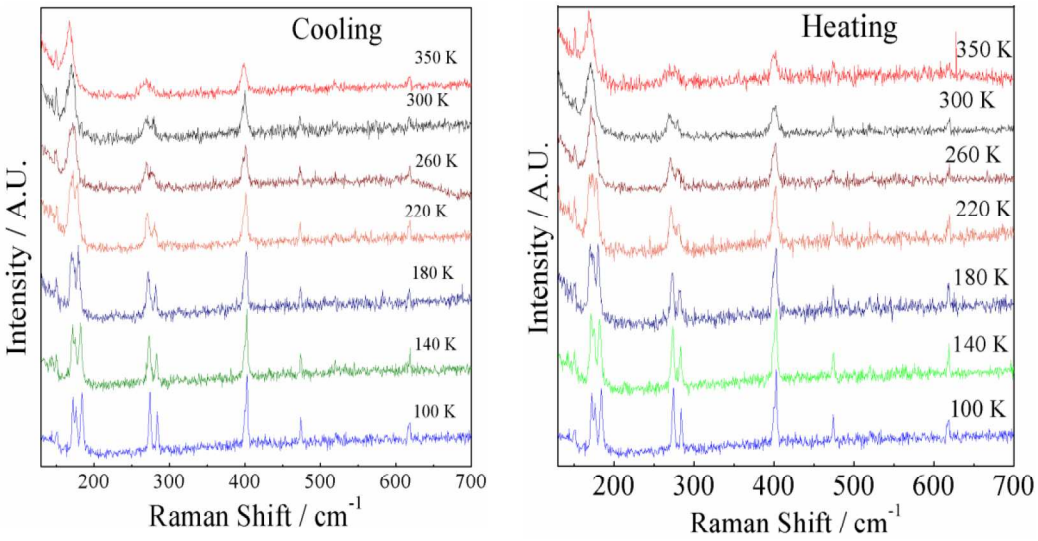

(a) (b)

Figure 3.4 Temperature evolutions of lattice modes in anilinium chloride.

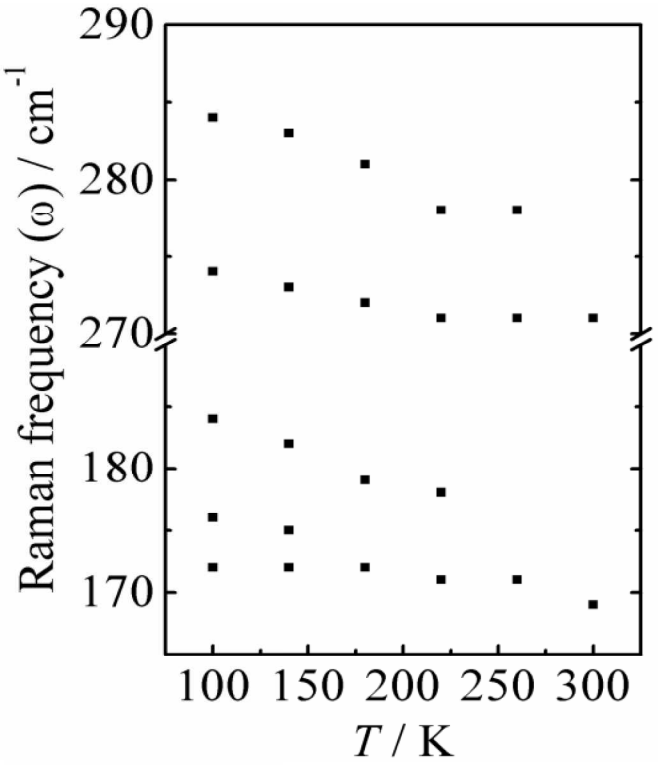

Figure 3.5 Raman frequencies as a function of temperature.

In present case, with the clear change of slope in ω versus T plot (as shown in Figure 3.5) at 260 K and around 300 K, indicates that there might be moderate change in the crystal symmetry accompanied by phase transition by lowering the temperature

[31]. Similar phase transitions are observed in case of temperature dependent Raman studies on ethyl ammonium chloride, where it undergoes enhanced hindered rotations in prototype phase [30]. Surprisingly, phase transitions in case of anilinium bromide and iodide were observed quite clearly using infrared spectroscopy and XRD measurements [32]. Figure 3.6 shows, clear emergence of mode centered around 2802 cm^{-1} due to R-NH_3^+ stretching vibrations overlapped and followed by number of combination bands by lowering the temperature to 100 K. Similar mode observed around 2570 cm^{-1} which might be of combination nature. These modes are very broad at RT suggesting appreciable motion of anilinium stretching vibrations due to hydrogen bonding. The comparatively lower frequency of the N-H (R-NH_3^+) stretching band in the spectra of anilinium chloride over its saturated anilinium analogue (cyclohexyl ammonium chloride at 2980 cm^{-1}) indicate that the hydrogen bonding is stronger in anilinium chloride. Surprisingly, these modes completely vanish if temperature is increased to 350 K. Consequently, there is one more phase transition between 300 K and 350 K in anilinium chloride. These vibrations are also reversible in nature. The mode in this region is due to extensive Fermi resonance with overtones and combination bands involving N-H bonding modes [28]. The transition between 300 K and 350 K were not detected in DSC study, even after repeated measurements, suggesting its sluggish nature. TG/DTA measurement clearly showed no mass loss or transitions up to 370 K. Infrared spectra on this compound showed, N-H stretching vibration around 3100 cm^{-1}, which was also observed in Raman spectra. On lowering temperature, below 350 K, this mode becomes much sharper, with splitting due to the degeneracy lifting. We believe that sharpening or emergence of R-NH_3^+ and splitting of the N-H stretching mode by lowering temperature is due to the presence of hydrogen bonding N-H···Cl and its prototype rotation a driving force for the torsional moment and hence a phase transition in a present monoclinic crystal system [33]. Also, sharpening of the N-H stretching mode with decreasing temperature is an indication of the ordering of the crystalline system below the transition temperature. Because of the temperature and volume dependence of the frequency of the stretching mode which, is considered as the phonon anharmonicity, the effect of the electron-phonon anharmonicities can be important on the mechanism of the order-disorder phase transition in an anilinium chloride.

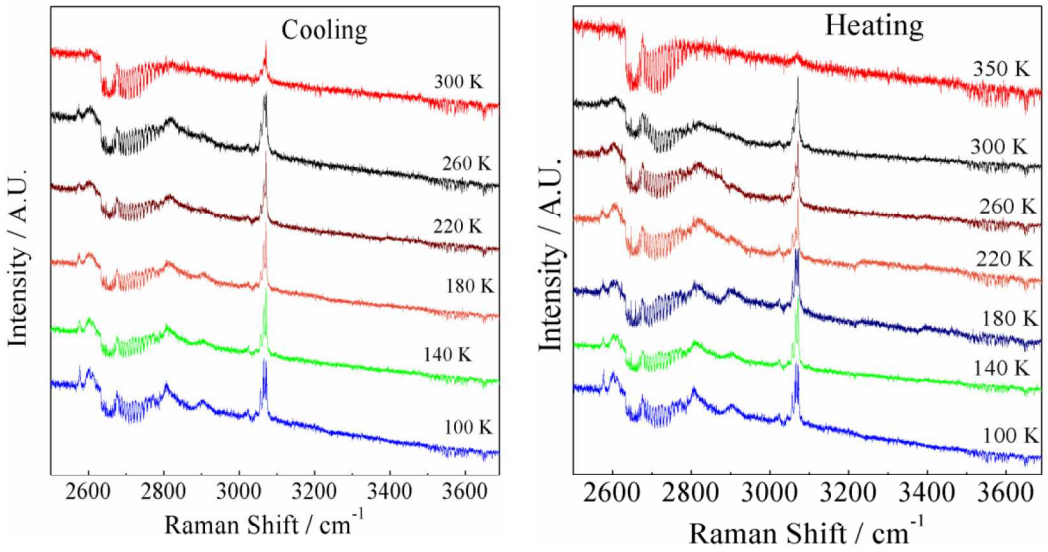

(a) (b)

Figure 3.6 Raman spectra in high frequency region as a function of temperature in anilinium chloride.

Temperature dependent Raman studies of 4-nitro anilinium chloride show five Raman modes at 127 cm^{-1}, 361 cm^{-1}, 398 cm^{-1}, 532 cm^{-1} and 633 cm^{-1} respectively in the low frequency region below 700 cm^{-1} at RT. These Raman modes are intense in lattice mode regions and carry out important information about dynamic of the transition. With lowering of the temperature Raman modes below 127 cm^{-1} revealed the clear emergence of two Raman modes centered around 100 cm^{-1} and 115 cm^{-1} between 260 K - 300 K. The other two Raman modes at 361 cm^{-1} and 532 cm^{-1} shows increase in the Rayleigh wing. These Raman modes at 361 cm^{-1} and 532 cm^{-1} completely vanish between 260 K - 300 K, as shown in Figure 3.7 (a). The modes centered around 100 cm^{-1} and 115 cm^{-1} disappear and other modes at 361 cm^{-1} and 532 cm^{-1} reappear on increasing the temperature its clearly indicating the reversibility. This indicates temperature dependent Raman spectroscopy also shows the solid-solid phase transition between 260 K - 300 K for 4-nitro anilinium chloride. On the other hand temperature dependent Raman studies for 3-nitro anilinium chloride shows the linear increase in Raman mode at 106 cm^{-1} (350 K) to 117 cm^{-1} (100 K). The modes at 191 cm^{-1} shows clear peak splitting at 185 cm^{-1} and 201 cm^{-1} below the 300 K see Figure 3.7 (b).

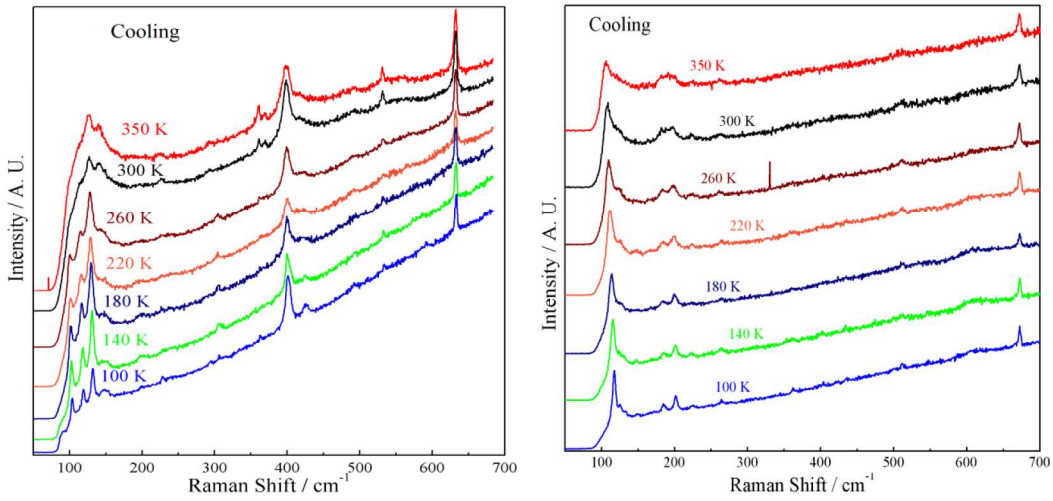

Figure 3.7 Temperature evolution of lattice modes in 4-nitro anilinium chloride (a) and 3-nitro anilinium chloride (b).

3.3.5 Thermal Analyses

3.3.5.1 Thermogravimetry/differential thermal analysis (TG/DTA)

TG/DTA thermogram represent most of the OACSs showed mass loss for OACs along with chloride anion, but in some cases mass loss for hydrochloride was observed first. Before the complete evaporation of hydrochloride, mass loss for organic amine get started (Table 3.3). DTA revealed endothermic peak for all OACSs (except benzilinium chloride and methyl ammonium chloride) due to thermal decomposition (Figure 3.8). DTA of some OACSs shows transition before the decomposition temperature, due to solid-liquid phase transitions (Figure 3.9). On the other hand in some cases OACSs shows mass loss without solid-liquid phase transition (Figure 3.10). DTA of 4-chloro benzilinium chloride shows the peak at 407.3 K, which indicates the evaporation of water molecule as shown in Figure 3.10 (b). The water molecule forms O-H···Cl hydrogen bonds, generating layers lying parallel to the *bc* plane [20]. In 4-chloro benzilinium chloride salt, water molecule lies on a crystallographic twofold axis. DTA for benzilinium chloride showed two transitions at 418.1 K and 476.5 K before the decompositions, due to solid-solid (418.1 K) and solid-liquid phase transition (476.5 K) see Figure 3.11.

Table 3.3 Paths of thermal decomposition in OACSs

Compounds	Tempe-rature [K]	Possibility	Moss Loss Theory [%]	Moss Loss Found [%]	Remains
NH_3HCl	571.8	NH_3HCl	100.00	99.65	-
$C_6H_5NH_3HCl$	474.0	$C_6H_5NH_3HCl$	100.00	99.97	-
4-F-$C_6H_4NH_3HCl$	468.2	4-F-$C_6H_4NH_3HCl$	100.00	99.87	-
4-Cl-$C_6H_4NH_2HCl$	473.1	4-Cl-$C_6H_4NH_2HCl$	100.00	99.59	-
3-Cl-$C_6H_4NH_2HCl$	450.8	3-Cl-$C_6H_4NH_2HCl$	100.00	99.73	-
4-NO_2-$C_6H_4NH_2HCl$	420.6	HCl	20.90	20.25	4-NO_2-$C_6H_4NH_2$
	516.1	4-NO_2-$C_6H_4NH_2$	79.10	79.21	-
3-NO_2-$C_6H_4NH_2HCl$	465.9	3-NO_2-$C_6H_4NH_2HCl$	100.00	100.00	-
$C_6H_5CH_2NH_2HCl$	544.5	$C_6H_5CH_2NH_2HCl$	100.00	100.00	-
4-Cl-$C_6H_4CH_2NH_2HCl.½H_2O$	407.3	H_2O	4.25	4.99	4-Cl-$C_6H_4CH_2NH_2HCl$
	539.9	4-Cl-$C_6H_4CH_2NH_2HCl$	98.68	90.79	-
(R)-$C_6H_5CH(CH_3)NH_2HCl$	535.0	(R)-$C_6H_5CH(CH_3)NH_2HCl$	100.00	99.57	-
(S)-$C_6H_5CH(CH_3)NH_2HCl$	542.5	(S)-$C_6H_5CH(CH_3)NH_2HCl$	100.00	98.82	
(R)-4-Cl-$C_6H_4CH(CH_3)NH_2HCl$	493.7	HCl	18.99	9.27	(R)-4-Cl-$C_6H_4CH(CH_3)NH_2$
	521.4	(R)-4-Cl-$C_6H_4CH(CH_3)NH_2$	81.01	91.93	-
(S)-4-Cl-$C_6H_4CH(CH_3)NH_2HCl$	492.6	HCl	18.99	14.44	(S)-4-Cl-$C_6H_4CH(CH_3)NH_2$
	538.8	(S)-4-Cl-$C_6H_4CH(CH_3)NH_2$	81.01	84.70	-
(R)-$C_6H_5CH(C_2H_5)NH_2HCl$	526.8	(R)-$C_6H_5CH(C_2H_5)NH_2HCl$	100.00	99.71	-
(S)-$C_6H_5CH(C_2H_5)NH_2HCl$	523.6	(S)-$C_6H_5CH(C_2H_5)NH_2HCl$	100.00	97.72	-
CH_3NH_2HCl	508.5	HCl	54.06	48.13	CH_3NH_2
	556.0	CH_3NH_2	45.94	51.87	-
$HClH_2NC_2H_4NH_2HCl$	603.4	$HClH_2NC_2H_4NH_2HCl$	100.00	96.62	-
$C_3H_7NH_2HCl$	544.6	$C_3H_7NH_2HCl$	100.00	96.62	-
(R)-1,2-$CH_3CH(NH_3)CH_2NH_32HCl$	605.3	(R)-1,2-$CH_3CH(NH_3)CH_2NH_32HCl$	100.00	98.17	-
(S)-1,2-$CH_3CH(NH_3)CH_2NH_32HCl$	579.5	HCl	50.67	71.86	(S)-1,2-$CH_3CH(NH_3)CH_2NH_3$
	637.1	(S)-1,2-$CH_3CH(NH_3)CH_2NH_3$	49.33	25.31	-
$C_4H_9NH_2HCl$	488.0	HCl	33.94	17.65	$C_4H_9NH_2$
	543.2	$C_4H_9NH_2$	66.06	80.14	-
(S)-$CH_3CH_2CH(CH_3)NH_2HCl$	475.1	HCl	33 .31	49.01	(S)-$CH_3CH_2CH(CH_3)NH_2$
	547.9	(S)-$CH_3CH_2CH(CH_3)NH_2$	66.69	50.99	-
2-Adamantyl-NH_2HCl	483.3	2-Adamantyl-NH_2HCl	100.00	99.57	-

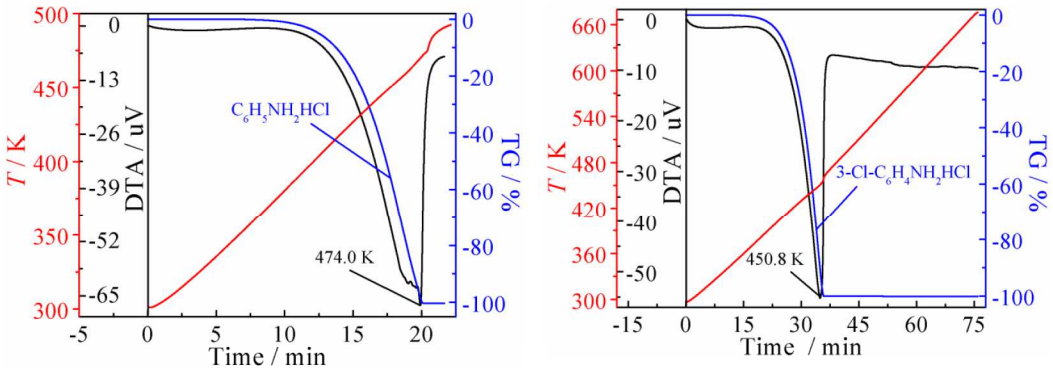

(a) (b)

Figure 3.8 TG/DTA thermogram for anilinium chloride (a) and 3-chloro anilinium chloride (b).

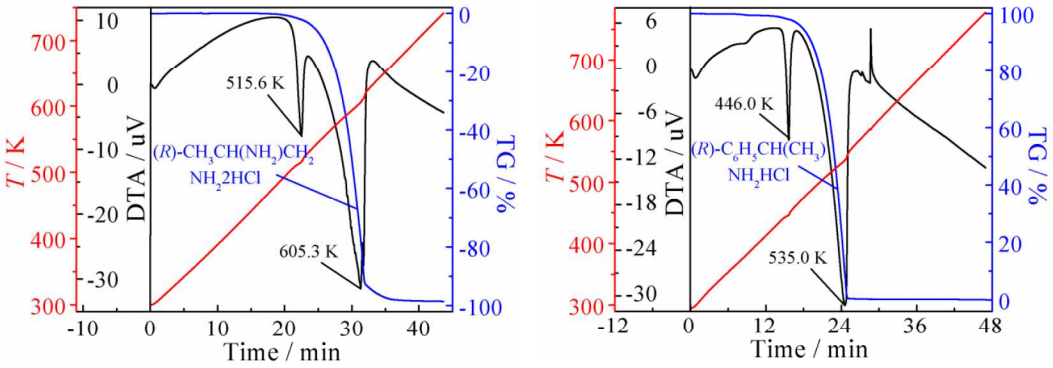

(a) (b)

Figure 3.9 TG/DTA thermogram for (*R*)-1,2-diammonium propane dichloride (a) and (*R*)-methyl benzilinium chloride (b).

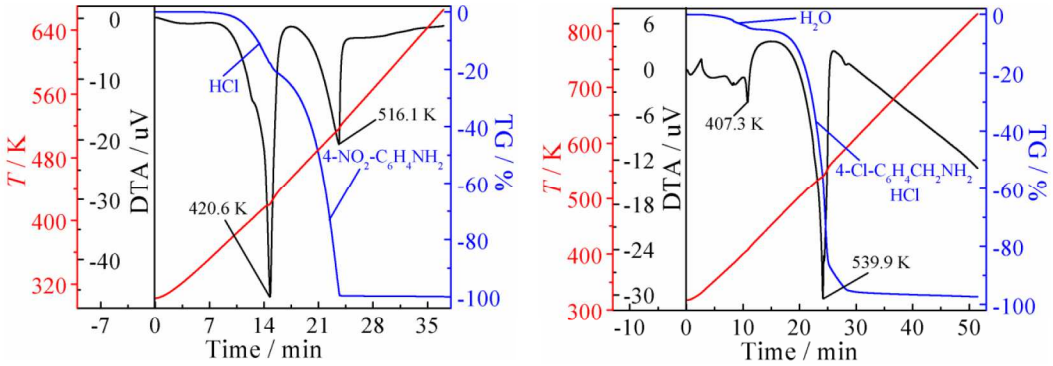

(a) (b)

Figure 3.10 TG/DTA thermogram of 4-nitro anilinium chloride (a) and 4-chloro benzilinium chloride (b).

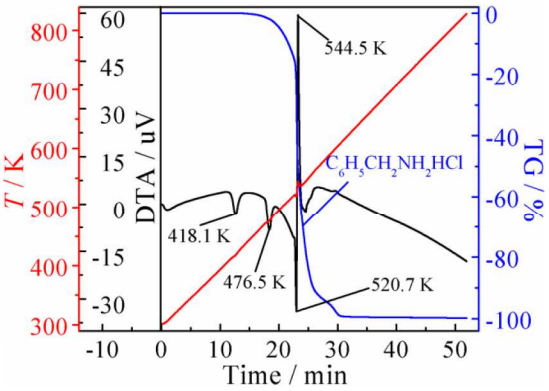

Figure 3.11 TG/DTA thermogram for benzilinium chloride.

3.3.5.2 Differential Scanning Calorimetry (DSC)

TG/DTA thermogram represents no mass loss till transition temperature reached in DSC for all OACSs. Enthalpies as well as transition temperatures have been reported for a number of substituted *n*-alkyl ammonium halides [4]. However, not much data has been reported for aromatic ammonium chlorides. The literature search for anilinium chloride has not shown any signature of phase transitions using infrared spectroscopy and powder XRD study. Surprisingly, Taguchi and Cabana were observed phase transitions for anilinium bromide and iodide using XRD and infrared spectra [14,32]. Therefore, we have preferred different substituent on OACSs (aromatic/aliphatic). The measured enthalpies and transition temperatures (153 K - 453 K) for the salts of OACSs are given in Table 3.4, for both increasing and decreasing directions of temperature scan. Interestingly anilinium chloride has shown exothermic transition at 245.35 K (0.29 J g^{-1}) during cooling DSC study as shown in Figure 3.12. After addition of any substituent on aromatic ring (except 3-nitro anilinium chloride) there is no solid-solid phase transition [Figure 3.13 (a)]. Similarly, benzilinium chloride shows two endothermic peaks at 404.83 K (-1.00 J g^{-1}) and 415.06 K (-45.09 J g^{-1}), characteristics for solid-solid phase transition. An exothermic peak, at 389.08 K (1.25 J g^{-1}), is characteristics for solid-solid phase transition and no transition was observed for 4-chloro benzilinium chloride see Figure 3.13 (b). Again (*R*)- and (*S*)-methyl benzilinium chloride, (*R*)- and (*S*)-ethyl benzilinium chloride shows one reversible solid-solid phase transition, but (*R*)- and (*S*)-4-chloro methyl benzilinium chloride are not shows any signature of solid-solid phase transition [Figure 3. 14 (a), (b), (c) and (d)]. Thus the addition of substituent on the aromatic

ring it is observed that there is no solid-solid phase transitions in OACSs, while the addition of substituent on benzylic position shows solid-solid phase transition see Table 3.4. These results are representing that addition of substituent on aromatic ring makes it hindered for free rotation of ammonium groups.

Table 3.4 DSC studies on OACSs

Compounds	**Phase Transition**			
	Heating		**Cooling**	
	Temperature [K]	**Enthalpy [J g^{-1}]**	**Temperature [K]**	**Enthalpy [J g^{-1}]**
Ammonium chloride	243.33	-13.40	237.56	20.42
	258.41	-9.67		
Anilinium chloride			245.35	0.29
4-Fluoro anilinium chloride	No transition observed			
4-Chloro anilinium chloride	No transition observed			
3-Chloro anilinium chloride	No transition observed			
4-Nitro anilinium chloride	No transition observed			
3-Nitro anilinium chloride	385.46	-69.24	357.26	54.16
Benzilinium chloride	404.83	-1.00	389.08	1.25
	415.06	-45.09		
4-Chloro benzilinium chloride	No transition observed			
(*R*)-Methyl benzilinium chloride	404.46	-2.71	389.63	1.06
(*S*)-Methyl benzilinium chloride	404.21	-1.93	389.06	0.87
(*R*)-4-Chloro methyl benzilinium chloride	No transition observed			
(*S*)-4-Chloro methyl benzilinium chloride	No transition observed			
(*R*)-Ethyl benzilinium chloride	403.83	-2.27	388.83	0.99
(*S*)-Ethyl benzilinium chloride	405.08	-4.14	389.34	2.03
Methyl ammonium chloride	216.67	-9.39		
	229.52	-17.17	217.73	15.75
	259.61	-38.99	208.85	43.59
Ethyl ammonium chloride	No transition observed			
1,2-Diammonium ethane dichloride	421.96	-76.41	318.20	29.92
n-Propyl ammonium chloride	189.62	-12.73	181.95	13.49
	225.58	-7.39	199.96	4.63
	406.35	-54.64	349.56	52.57
(*R*)-1,2-Diammonium propane dichloride	406.20	-2.71	388.87	1.18
(*S*)-1,2-Diammonium propane dichloride	404.46	-2.71	389.34	0.91
1,3-Diammonium propane dichloride	No transition observed			
n-Butyl ammonium chloride	235.09	-5.33		
	240.78	-21.09	211.70	5.23
	258.38	-17.88	224.62	33.61
(*S*)-2-Butyl ammonium chloride	No transition observed			
2-Amino benzothiazolinium chloride	No transition observed			
2-Adamantanamidinium chloride	No transition observed			

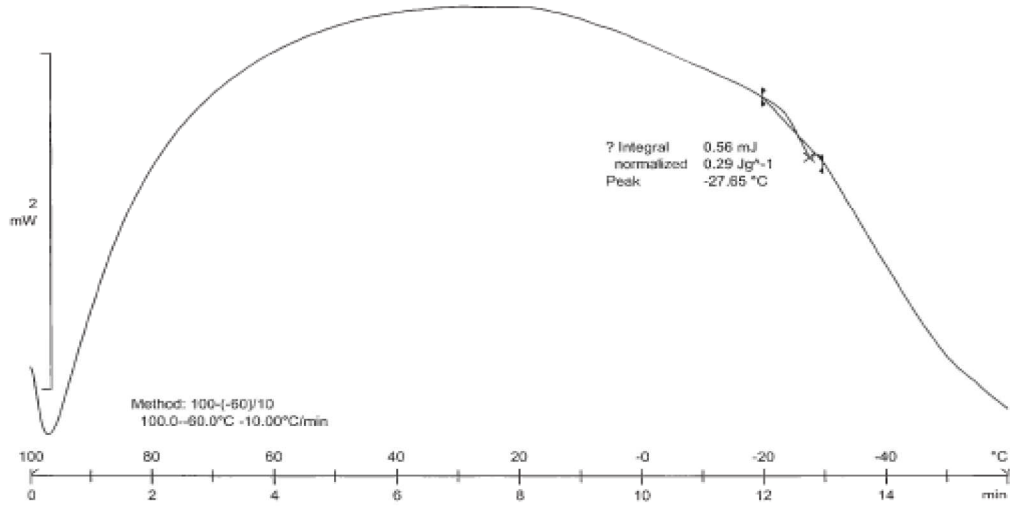

Figure 3.12 DSC thermogram of anilinium chloride showing phase transition.

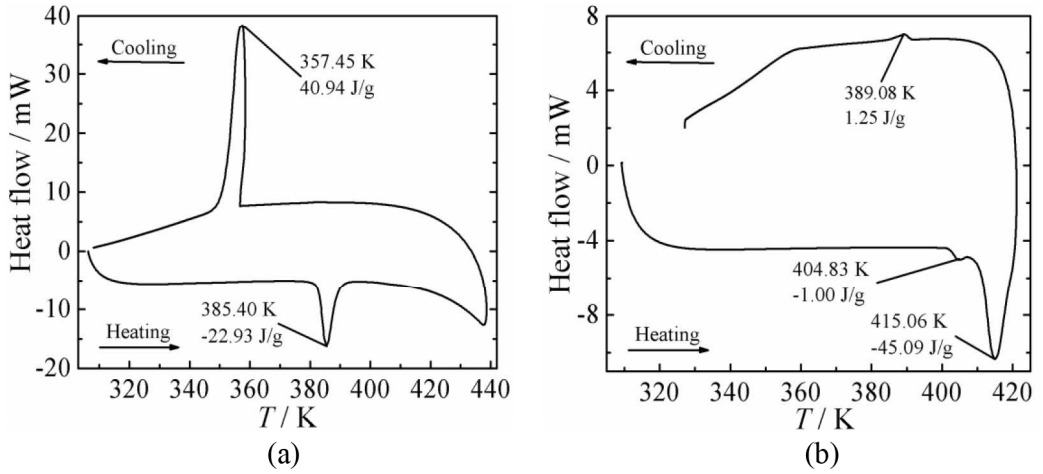

Figure 3.13 DSC thermogram of 3-nitro anilinium chloride (a) and benzilinium chloride (b), showing reversible phase transition.

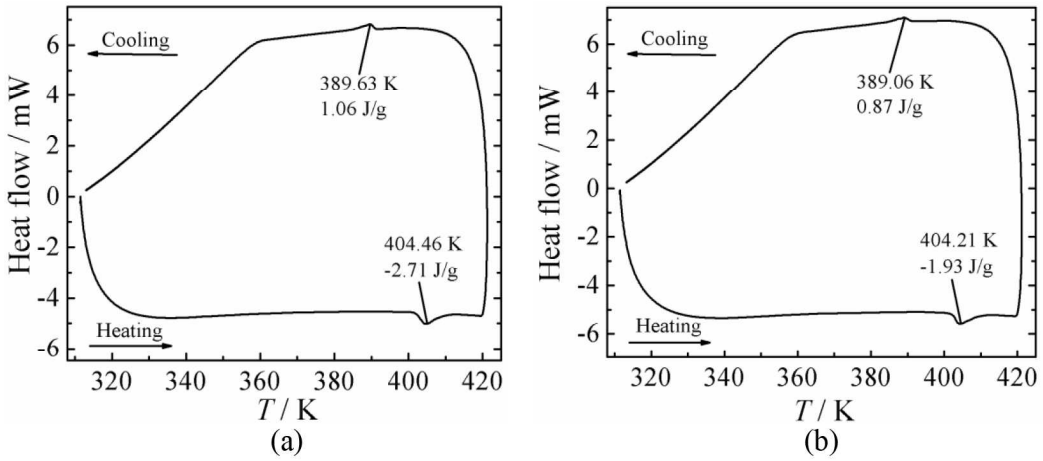

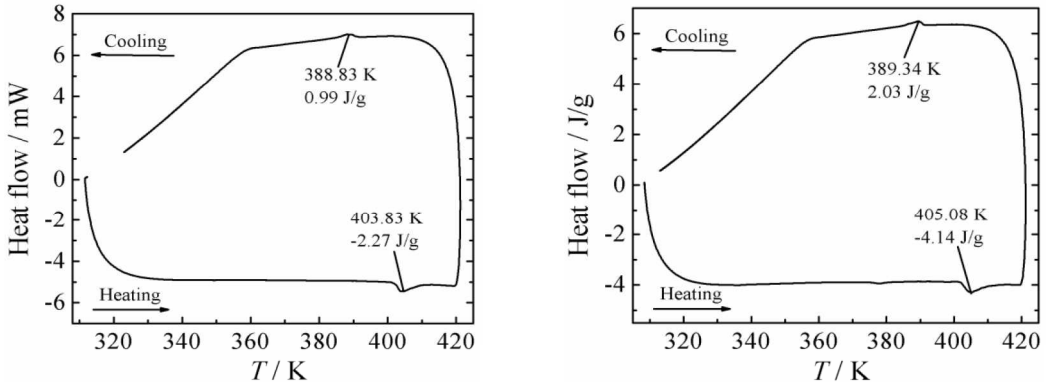

Figure 3.14 DSC thermogram of (*R*)- and (*S*)-methyl benzilinium chloride (a); (b), and (*R*)- and (*S*)-ethyl benzilinium chloride (c) and (d), showing reversible phase transition.

On the other side, aliphatic OACSs, ammonium chloride, (*R*)- and (*S*)-1,2-diammonium propane dichloride, *n*-butyl ammonium chloride and *n*-propyl ammonium chloride have reveled one, two, four reversible solid-solid phase transition respectively. No transitions were observed for (*S*)-2-butyl ammonium chloride, 2-amino benzothiazolium chloride and 2-Adamantanamidinium chloride using DSC thermogram. For homologous series such as *n*-alkanes, the alternation of transition temperatures, temperatures of fusion and enthalpies, etc., as a function of the number of atoms in the chain is well known [34]. The alternation in melting points is attributed to melting from different crystal structures of the odd and even members of the series, even though in many cases structures are not known. In reported literature chloride salts for *n*-alkanes, one or two transitions have available up to C_7, except C_1 and C_6, three or more than three transitions are observed for higher than C_7 [35]. Interestingly for C_3 we have observed three endothermic peaks at 189.62 K (-12.73 J g^{-1}), 225.58 K (-7.39 J g^{-1}) and 406.35 K (-54.64 J g^{-1}) while heating and three exothermic peaks at 181.95 K (13.49 J g^{-1}), 199.96 K (4.63 J g^{-1}) and 349.56 K (52.57 J g^{-1}) while cooling characteristics for solid-solid phase transitions as shown in Figure 3.15. These results are in contradiction with the data present in literature, where C_3 has only two phase transitions at 188 K and 408 K using DSC thermogram [35]. While in case of C_1 and C_4 transition is observed similar as reported in literature [35]. In bifunctional, structure of 1,2-diammonium ethane dichloride and 1,3-diammonium propane dichloride were first obtained by Ashida and Hirokawa [36]. The one unit cell contains half 1,2-diammonium ethane cations and one chloride anion for 1,2-

diammonium ethane dichloride and four molecules for 1,3-diammonium propane dichloride, with one cation is surrounded by six chloride anions [37]. 1,2-diammonium ethane dichloride shows one endothermic peak at 421.96 K (-76.41 J g^{-1}) while heating and one exothermic peak at 318.20 K (29.92 J g^{-1}) while cooling (Figure 3.16). 1,3-Diammonium propane dichloride does not show any signature of phase transition in DSC thermogram. The crystal structure (*R*)- and (*S*)-1,2-diammonium propane dichloride are not known in literature. DSC study shows endothermic peaks at 406.20 K (-2.71 J g^{-1}), 404.46 K (-2.71 J g^{-1}) while heating and exothermic peaks at 388.87 K (1.18 J g^{-1}), 389.34 K (0.91 J g^{-1}) while cooling for (*R*)- and (*S*)-1,2-diammonium propane dichloride as shown in Figure 3.17. All these transitions are reversible in nature because, if the same compound was scanned more than once, we obtained same peak without any observable change. HT transitions are assigned to the rotational transition, rather than the LT transition. Freezing disorder could be explained by the differences between the first and subsequent DSC thermogram.

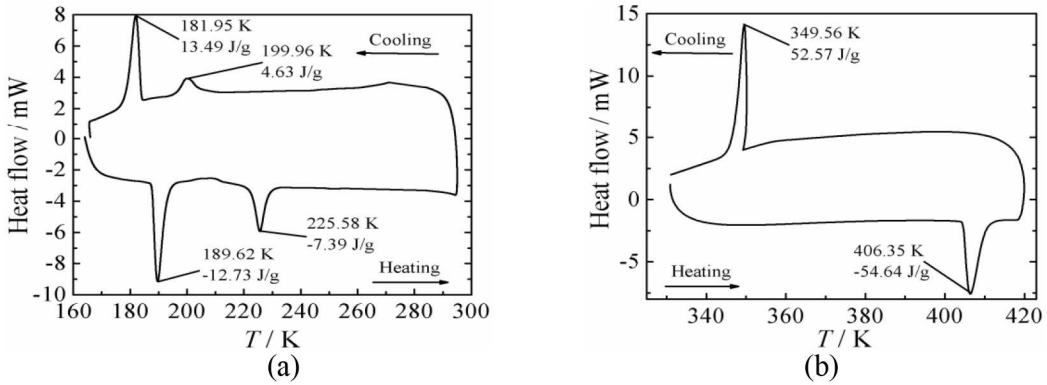

Figure 3.15 DSC thermogram of *n*-propyl ammonium chloride at LT (a) and HT (b), showing the reversible phase transition.

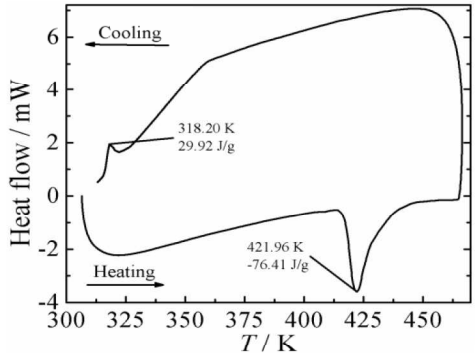

Figure 3.16 DSC thermogram of 1,2-diammonium ethane dichloride showing the reversible phase transition.

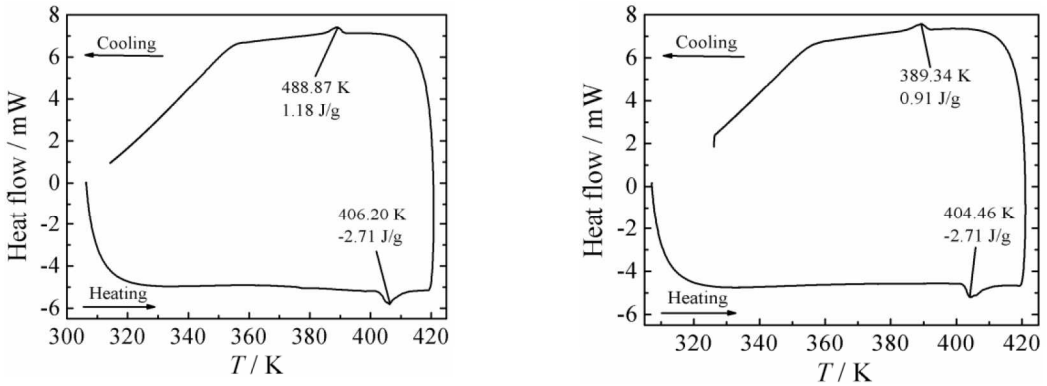

Figure 3.17 DSC thermogram of (*R*)- and (*S*)-1,2-diammonium propane dichloride (a) and (b), showing the reversible phase transition.

3.4 Conclusion

- We have synthesized and characterized twenty two OACSs using FT-IR, ^{1}H NMR.
- OACSs investigated for possible structural phase transitions using TG/DTA measurements, DSC study and wherever necessary temperature dependent Raman study was carried out.
- TG/DTA measurements showed different degradation paths in OACSs, where organic amine and hydrochloride gas compete for the 'initial' loss.
- Most of the OACSs are stable up to 370 K; monoammonium chloride salts showed mass loss below 500 K (below 400 K for anilinium chloride and derivative, and above the 400 K for *n*-alkyl, benzilinium chloride and derivative) and diammonium chloride salts above the 500 K. There is no constant change observed for substituent (electron withdrawing/donating) on aromatic ring for present set.
- DSC studies on aromatic OACSs showed no observation of solid-solid phase transition when any substituent present on aromatic ring (except 3-nitro anilinium chloride).
- Thermal behaviors proved that aliphatic OACSs undergo order-disorder phase transition at different temperatures, which are reversible in nature.
- The anilinium chloride has two solid-solid phase transitions; one around 260 K and the other between 300 K - 350 K. 4-nitro anilinium chloride has one solid-

solid phase transition between 260 K - 300 K conformed by temperature dependent Raman spectroscopy. While 3-nitro anilinium chloride show splitting in Raman mode with lowering temperature.

References

[1] H. Hagemann, H. Bill, *J. Chem. Phys.* **1984**, *80*, 111-118.

[2] F. Awwadi, R. D. Willet, B. Twamley, R. Schneider, C. P. Landee, *Inorg. Chem.* **2008**, *47*, 9327-9332.

[3] P. S. Ghalsasi, K. Inoue, *Polyhedron* **2009**, *28*, 1864-1867.

[4] O. Yamamuro, M. Oguni, T. Matsuo, H. Suga, *Thermochim. Acta* **1986**, *98*, 327-338.

[5] R. S. Seymour, A. W. Pryor, *Acta Cryst. B* **1970**, *26*, 1487-1491.

[6] R. Mokhlisse, M. Couzi, P. L. Loyzance, *J. Phys. C Solid State Phys.* **1983**, *16*, 1367-1384.

[7] M. Stammler, *J. Inorg. Nucl. Chem.* **1967**, *29*, 2203-2221.

[8] G. H. Goldschmidt, D. G. Hurst, *Phys. Rev.* **1951**, *83*, 88-94.

[9] H. A. Levy, S. W. Peterson, *Phys. Rev.* **1952**, *86*, 766-770.

[10] F. Jellinek, *Acta Cryst.* **1958**, *11*, 626-631.

[11] V. Migliorati, P. Ballirano, L. Gontrani, A. Triolo, R. Caminiti, *J. Phys. Chem. B* **2011**, *115*, 4887-4899.

[12] J. Tsau, D. F. R. Gilson, *J. Phys. Chem.* **1968**, *72*, 4082-4085.

[13] M. Gordon, E. Stenhagen, V. Vand, *Acta Cryst.* **1953**, *6*, 739-741.

[14] A. Cabana, C. Sandorfy, *Can. J. Chem.* **1962**, *40*, 622-629.

[15] S. T. Rao, M. Sundaralingam, *Acta Cryst. B* **1969**, *25*, 2509-2515.

[16] J. D. Bernal, *Nature* **1932**, *129*, 870.

[17] G. Ploug-Sørensen, E. K. Andersen, *Acta Cryst. C* **1986**, *42*, 1813-1815.

[18] G. Ploug-Sørensen, E. K. Andersen, *Acta Cryst. B* **1982**, *38*, 671-673.

[19] G. Ploug-Sørensen, E. K. Andersen, *Acta Cryst. C* **1985**, *41*, 613-615.

[20] S. Souissi, W. S. Sta, S. S. Al-Deyab, M. Rzaigui, *Acta Cryst. E* **2010**, *66*, 1627.

[21] M. Colapietro, A. Domenicano, G. Portalone, *Acta Cryst. B* **1982**, *38*, 2825-2529.

[22] C. J. Brown, *Acta Cryst.* **1949**, *2*, 228-232.

[23] K. Raatikainen, M. Cametti, K. Rissanen, *Bull. J. Org. Chem.* **2010**, *6*, 1-13.

[24] M. V. King, W. N. Lipscomb, *Acta Cryst.* **1950**, *3*, 227-230.

[25] W. Dultz, *J. Chem. Phys.* **1976**, *65*, 2812-2816.

[26] A. D. Bruce, W. Taylor, A. F. Murray, *J. Phys. C* **1980**, *13*, 483-504.

[27] E. K. Gibson, J. M. Winfield, K. W. Muir, R. H. Carr, A. Eaglesham, A. Gavezzotti, D. Lennon, *Phys. Chem. Chem. Phys.* **2010**, *12*, 3824-3833.

[28] C. N. R. Rao, S. Ganguly, H. R. Swamy, I. A. Oxton, *J. Chem. Soc. Faraday Trans.* **1981**, *277*, 1825-1836.

[29] M. K. Marchewka, A. Pietraszko, *J. Phys. Chem. Solids* **2005**, *66*, 1039-1048.

[30] P. S. R. Prasad, *J. Phys. Chem.* **1996**, *100*, 888-890.

[31] **A. K. Vishwakarma**, P. Ghalsasi, P. S. Ghalsasi, *Phys. Status Solidi B* **2011**, 1-5.

[32] I. Taguchi, *Bull. Chem. Soc. Jpn.* **1961**, *34*, 392-395.

[33] M. -H. Herzog-Cance, D. J. Jones, R. Mejjad, J. Rozière, J. Tomkinson, *J. Chem. Soc. Faraday Trans.* **1992**, *88*, 2275-2281.

[34] R. Lippman, R. Rudman, *J. Thermal Anal.* **1976**, *9*, 229-231.

[35] J. Tsau, D. F. R. Gilson, *J. Phys. Chem.* **1968**, *72*, 4082-4085.

[36] T. Ashida, S. Hirokawa, *Bull. Chem, Soc, Jpn.* **1963**, *36*, 704-707.

[37] A. M. Amado, J. C. Otero, M. P. M. Marques, L. A. E. B. de Carvalho, *Chem. Phys. Chem.* **2004**, *5*, 1837-1847.